Proceedings of the International Conference on Oxide Materials for Electronic Engineering, May 29–June 2, 2017, Lviv

Luminescent Spectroscopy of the Yb^{3+} Ions in the $PbWO_4$ Crystal

O. Chukova* and S.G. Nedilko

Physics Faculty, National Taras Shevchenko University of Kyiv, 4-b, acad. Hlushkov Ave., 03680, Kyiv, Ukraine

Luminescent properties of the $PbWO_4$ crystals undoped and doped with the Yb^{3+} ions were studied. Emission spectra of the crystals consist of broadband matrix emission in 350–750 nm spectral range and narrow spectral lines caused by inner electron transitions in the impurity Yb^{3+} ions in 920–1040 nm spectral range. Analysis of the linear spectra has shown that Yb^{3+} ions form two types of emission centres. Structures of these centers are discussed taking into account possibility of the impurity ions incorporation in different positions (Pb and W sites) in the crystal lattice. Effects of the Yb^{3+} impurities on matrix emission were studied. Transfer of excitation energy from matrix to the Yb^{3+} decreases intensity of the red band of matrix emission. The Yb^{3+} impurities also increase intensity of the blue band by formation of additional Yb^{3+}-induced channel of excitation of this band. The described effects of Yb^{3+} doping on properties of matrix emission are caused by the Yb^{3+} ions arranged in Pb positions.

DOI: 10.12693/APhysPolA.133.918

PACS/topics: 61.72.Ji, 78.55.Hx

1. Introduction

Family of tungstate crystals brings one of the largest sets of luminescent materials in the technique of high energy particles registration and in the technique of tomography devices ($PbWO_4$, $CdWO_4$, $CaWO_4$) [1–3]. Single crystal tungstates are now applied in the technique of laser radiation frequency shifting using the Raman scattering stimulation ($CaWO_4$, $BaWO_4$, $SrWO_4$, $PbWO_4$) [4–7]. Tungstate compounds are also successfully used in many others research and technology areas. Therefore, development of their characteristics is important task for mentioned applications [8–10]. The main method used for achievement of the tungstates crystals optimal operation performance is their doping with impurity ions, especially with rare earth (RE) ions, and annealing of the grown crystals in various atmospheres, e.g. oxygen, argon, air [11–14]. Therefore, knowledge about luminescence mechanisms and excitation energy transfer between the RE impurity centers and matrix is very important. Properties of the $PbWO_4$ (PWO) crystals and of the PWO nanoparticles doped with various RE^{3+} ions were intensively studied previously. Especially, it concerns Eu^{3+}, Pr^{3+}, Tb^{3+}, Nd^{3+} impurities [15–18]. The luminescence properties of Yb^{3+} ions doped PWO were previously reported only episodically and poorly [5, 19–21]. In this work, we carry out study of luminescence properties of the Yb^{3+} ions impurity in the PWO matrix and investigate mutual correlations in behaviour of matrix and impurity emission.

The Yb^{3+} ions were chosen at this study for two reasons: their spectra do not overlap with matrix emission and these ions are actual for such tungstate applications as laser crystals and luminescent converters of solar light. Luminescence properties of the Yb^{3+} ions in PWO crystals were briefly reported previously in the papers devoted to study of various RE^{3+} ions influence on properties of the PWO emission [19, 20]. Effects of annealing on absorption and X-rays luminescence spectra of the Yb^{3+}-doped PWO crystals were considered in [5, 21]. These papers reported also excited at 940 nm and at room temperature the Yb^{3+} emission spectra which consist of a broad band from 950 to 1100 nm with a maximum at 1003 nm and a narrow peak at 978 nm. It was supposed that Yb^{3+} ions occupy the Pb^{2+} sites and induce an positive excess charge +1 into the crystal, which is compensated by Pb vacancies (two Yb^{3+} ions at two Pb^{2+} sites on one Pb vacancy). Other results showed the formation of two types emission centers for other RE^{3+} ions in PWO crystals, e.g, Nd^{3+}, Eu^{3+}, Gd^{3+}, Tb^{3+} [18, 22–24]. Noted discrepancy maybe related with some peculiarities of the Yb^{3+} incorporation into PWO lattice. Besides, a lack of experimental data could be an origin of this discrepancy, too, taking into account that only room temperature emission spectra were reported for the IR range [5, 20, 21]. Therefore, the first goal of this paper is to clarify a number of the Yb^{3+} emission centers in the PWO crystals using low temperature study of IR luminescence. Identification of possible correlations between manifestation of the PWO matrix luminescence and behavior of the Yb^{3+} impurity luminescence in this matrix is the second goal of this paper.

2. Experiment

The lead tungstate crystals were grown by the Czochralski method using the Crystal-617 equipment at Physics Faculty of the Ivan Franko National University of Lviv, Ukraine. The blend was synthesized from lead, tungsten and corresponding RE oxides. The impurity concentrations in the blend were 5×10^{-2} wt%. The

*corresponding author; e-mail: chukova@univ.kiev.ua

rectangular $5 \times 10 \times 10$ mm^3 bricks used for the study were cut from the central part of a crystal bulk. The samples studied in this work were not annealed in any specific atmosphere.

Luminescent measurements under UV excitation were carried out using synchrotron radiation at SUPERLUMI station at HASYLAB, Hamburg, Germany as it was described in [25, 26]. Excitation spectra of the IR luminescence were measured at R&D Laboratory "Spectroscopy of condensed state of matter" (Physics Faculty of the Taras Shevchenko National University of Kyiv) using radiation of power xenon lamp [27]. Excitation spectra were corrected on spectra of etalon sodium salicylate. Luminescence spectra were corrected for spectral sensitivity of the registering equipment.

3. Results

Emission spectra of the Yb^{3+}-doped PWO crystal at 10 K contain wide bands in 350–750 nm spectral range and narrow bands in the 970–1040 nm range (Fig. 1). Maxima of the wide band spectra at the short wavelength excitations (200–300 nm) are located at 445 nm (Fig. 1). Weak component with maximum at about 570 nm forms long wavelength tail of the spectra at those excitations. The spectra obtained at the long wavelength excitations (309–340 nm) have maxima at 510 nm (Fig. 1). The 970–1030 nm band is only observed for the Yb^{3+}-doped crystals at all applied excitations, but its relative contribution strongly depends on excitation wavelength (Fig. 1).

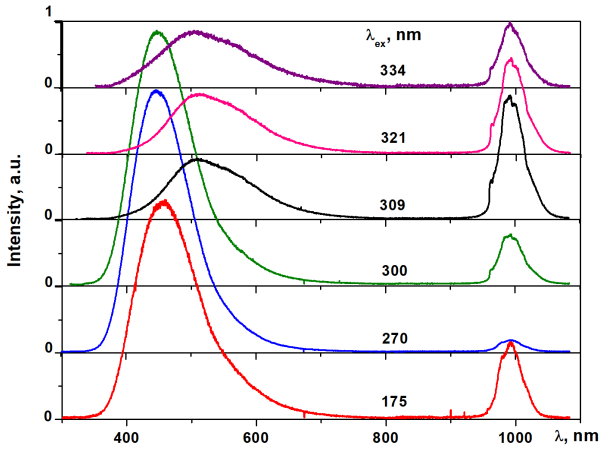

Fig. 1. Luminescence spectra of matrix and Yb^{3+} emission of the Yb^{3+}-doped PWO crystals at 10 K and various excitations, $d_{slits} = 2$ mm.

Experiments carried out with fine spectral slits of spectrometers (d_{slits}) revealed that the IR band consists of at least 8 narrow spectral lines (Fig. 2a). These lines can be divided on two types by dependence of their relative intensity on excitation wave length. We assigned the group of more intensive lines (978, 997, 999.5, and 1023 nm) to the first type of emission. These lines are intensive in the spectra obtained at the long wavelength excitations (300–340 nm). Their intensities significantly fall down at excitations with λ_{ex} <300 nm, whereas intensity of the rest lines does not depend on excitation wavelength. These lines have been assigned to the second type of emission. Noted that distinctive raise of intensity of the first type of lines correlates with the shift of maximum position of the wide band of visible emission from 445–455 nm, if λ_{ex} <300 nm, to 510 nm, if $\lambda_{ex} = 309$ nm.

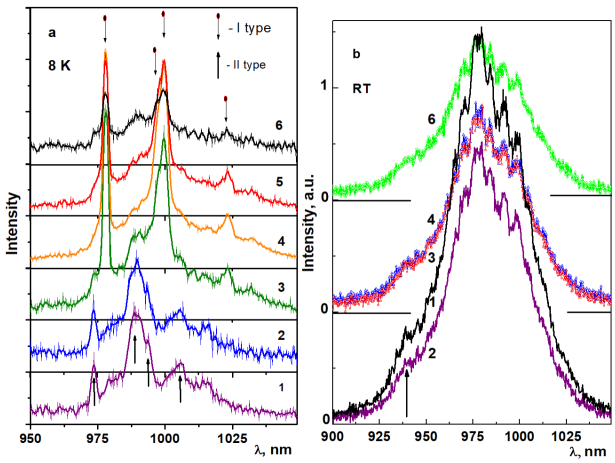

Fig. 2. Emission spectra of the Yb^{3+} ions in the PWO crystals in the range of f–f radiation transitions, at 8 K (a) and RT (b) $\lambda_{ex} = 175$ (1), 270 (2), 300 (3), 309 (4), 321 (5), 334 (6) nm, $d_{slits} = 0.2$ mm.

At room temperature, IR emission was observed in the 920–1040 nm spectral range (Fig. 2b). The spectra measured under various excitations are the same. They have only weakly resolved structure. Compared to the low temperature spectra, the IR emission at room temperature has additional band at about 940 nm (this band is marked by arrow in Fig. 2b).

Excitation spectra of the wide band emission have the sharp long wavelength edge and the sharp peak at near 296 nm; wide asymmetric bands in 150–220 and 220–290 nm spectral ranges and weak band in the 300–330 nm spectral range with maximum at about 320 nm. Excitation spectra of the IR emission ($\lambda_{em} = 990$ nm) in the used spectral range contain two bands with maxima at $\approx$ 235 and 305 nm. Shape of the latter band has complex character that evidences presence of at least two components at 305 and at about 320 nm (Fig. 3). Reflectance spectrum of the Yb^{3+}-doped PWO crystal consists of three bands in 150–270, 270–310, and 310–340 nm spectral ranges with maxima near 235, 292, and 315 nm, respectively (Fig. 3, curve 5). The most intensive 270–310 nm band is characterized by sharp long wave length edge and two shoulders at 282 and 296 nm.

4. Discussion

4.1. Impurity emission

The observed spectra of linear emission of the Yb^{3+}-doped PWO crystal in the 970–1040 nm range is caused by f–f transitions in the Yb^{3+} ions. This range belongs to the $^2F_{5/2} \rightarrow ^2F_{7/2}$ transitions [28–30]. The $^2F_{7/2}$ level in crystal field splits into 4 Stark components maximally.

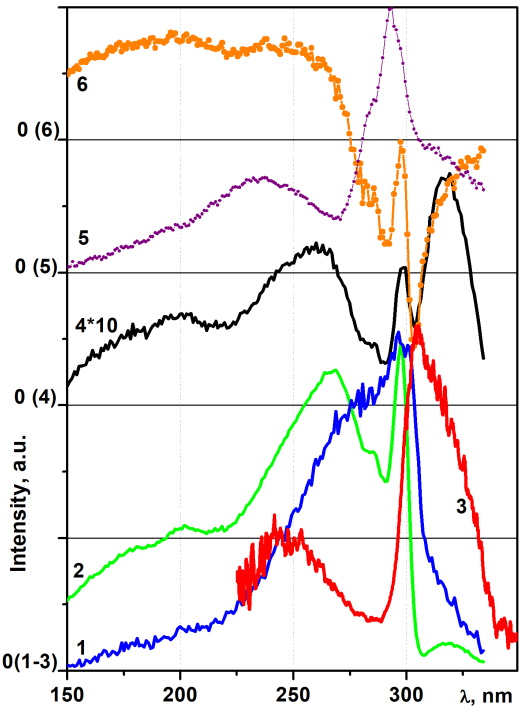

Fig. 3. Excitation (1–4) and reflectance (5) spectra of the un-doped (1) and Yb^{3+}-doped (2–5) PWO crystals at 10 K, λ_{em} = 400 (1, 2), 990 (3), 570 (4) nm and difference (6) between spectra 2 and 1 $I(6) = I(2) - I(1)$.

Observed for the crystals under study 8 spectral components can be easily divided into two groups of lines marked by different arrows in Fig. 2, and listed in Table I. Transitions from higher sub-levels of the $^2F_{5/2}$ manifold are not expected at 10 K. Usually, they are located at spectral ranges of higher energies: the nearest transition from higher level is expected at ≈ 920–940 nm [29, 30]. We have observed a weak band corresponding to the noted transition only in the spectra measured at room temperature (marked by an arrow in Fig. 2b).

TABLE I

Peak positions of Stark splitting components in the PL spectra of the $PbWO_4$–Yb^{3+} crystals

Peak positions		Types of the centres
λ [nm]	E [cm^{-1}]	
973.5	10270	**II**
978	10225	**I**
989	10110	**II**
994	10060	**II**
997	10030	**I**
999.5	10005	**I**
1006	9940	**II**
1023	9775	**I**

We assign the observed at 10 K two groups of lines to different types of emission centers formed by the impurity Yb^{3+} ions in the PWO crystal lattice (Fig. 4, Table I). According to Fig. 2, these centers have quite different intensity of emission. The II type of centers is characterized by intensity of luminescence by more than 10 times lower compared to the I type of centers (Fig. 2a). The observed significant differences between spectral properties of two types of centers formed by the Yb^{3+} ions are explained by different ways of the impurity ions incorporation into PWO crystal lattice. There are Yb^{3+} substitutions for Pb and W sites for the I and II type of centers, respectively. Possibility of such incorporation was shown previously for the PWO crystals doped with other RE^{3+} ions [13, 18, 31, 32]. Besides, it should be noted that probability of the RE ions arrangement in the tungsten sites is essentially lower than in the lead sites of PWO matrix. Therefore, concentration of the II types centers is smaller by tens times than concentration of the II types centers. This results in a lower emission intensity of the II type of centers compared to I type of centers (Fig. 2a). Moreover, these two types of centers possess different symmetry of the RE^{3+} ions (C_s and D_2 for I and II types, respectively) and impact of the crystal field. For example, the action of crystal field on impurity RE ions is higher for the II type of centers due to great difference between ionic radii of tungsten and impurity ions) [22]. Different symmetry and crystal field strength result in different energy distribution of the lines corresponded to I and II types of the centers (Fig. 4).

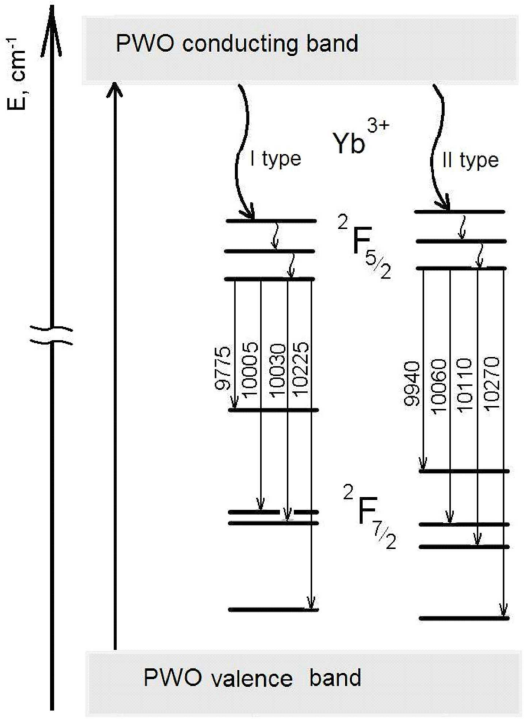

Fig. 4. Scheme of electron transitions responsible for the Yb^{3+} emission in the Yb^{3+}-doped PWO crystals.

4.2. Matrix emission

The observed wide bands in the 350–750 nm spectral range belong to matrix emission of the PWO crystals. This emission is complex and consists of strongly overlapping wide bands (Fig. 1). In particular, there are well known blue, green and orange-red luminescence bands, those have excitonic nature (blue and green bands) or caused by electron transition in defect local centers (orange-red bands) [32–36]. Relative contributions of these bands in the total spectra depend on excitation wavelength that leads to redistribution of shapes and maxima positions of the spectra measured at different excitations [36–39].

Matrix emission spectra of the RE^{3+}-doped crystals are shifted to the blue side compared with the spectra of un-doped crystal [38]. Taking into account well-known complex multi band character of the PWO matrix emission, we have considered that observed shift is caused by different contributions of various bands in the spectra of the doped and un-doped crystals. We have shown in our previous works that all emission spectra of the un-doped and RE-doped PWO crystals can be quite described with sum of several wide bands those are the same for various crystals [32, 38]. It was shown that relative contributions of the blue band in the total spectra are strongly increased for the RE^{3+}-doped crystals compared with the un-doped PWO crystals whereas the red band is more intensive in the spectra of the un-doped PWO crystals [38]. Effect of the RE ions on the blue emission can be a result of formation by the RE impurities of additional channel of energy transfer for creation of excitons or a result of common effect of the RE impurities on energy structure of the host lattice [32]. As for effects of the RE impurities on the PWO lattice structure, we should note that RE doping decreases content of oxygen vacancies [39–41] and increases in such a way contribution of the regular WO_4^{2-} groups, where the blue emission arises. The observed suppression of the red band in the Yb^{3+}-doped PWO crystals agrees with conclusion made previously that red emission is connected with lead vacancies [35], because the impurity RE ions significantly decrease content of the lead vacancies in the PWO crystal lattice.

4.3. Excitation

The excitation spectra of matrix emission can be divided on three spectral ranges those belong to different types of transitions. There are 150–270 nm range of matrix transitions containing wide spectral bands with two main maxima at about 180 and 270 nm; 270–308 nm range of exciton transitions containing sharp peaks at 303, 296, and 282 nm; 300–340 nm range of transitions in defects of the PWO matrix containing bands maximum at 320 nm [31–35]. Doping with the Yb^{3+} ions causes changes in the shapes of these bands. Difference between excitation spectra of matrix emission for the Yb^{3+}-doped and un-doped crystals is shown in Fig. 3, curve 6.

We noted above that there are two types of the Yb^{3+} emission centers, when the Yb^{3+} ions are located in the Pb and W positions, I and II types, respectively. Significant difference in neighbor surrounding of the Yb^{3+} centers must affect luminescence excitation processes. It is easy to see from Fig. 2a that emission of II type centers is better excited from the 150–270 nm spectral range, whereas emission of the I type centers is worse excited from this spectral range. We suppose that excitation energy absorbed in this range is mainly realized in the matrix emission (blue band) and the I type centers are characterized by higher efficiency of excitation energy transfer from 150–270 nm spectral range to the matrix.

On the other hand, the most intensive excitation band of the red matrix emission is located at the same range that most intensive excitation band of the Yb^{3+} IR emission (300–340 nm). This excitation band lies on absorption edge of the PWO matrix and corresponds to range of defect transitions (Fig. 3, curve 5). It is easy to see from Fig. 3 that behavior of curve 6 repeats main features of curve 4 that presents excitation spectra of the red band of matrix emission. As it was reported previously, relative intensity of the 309–334 nm excitation band is strongly decreased in the spectra of the RE^{3+}-doped crystals [32]. Its decrease correlates with suppression of the emission band at 635 nm in the Yb^{3+}-doped crystals [38]. At the same time, strong emission of the I type of Yb^{3+} centers (Figs. 1, 2, curves 4, 5) is excited in this range. Thus, we assume that excitation energy absorbed by matrix from the 309–334 nm band is realized within IR f–f intrinsic emission of the Yb^{3+} centres (I type centres with the Yb^{3+} ions in the Pb positions) that is followed by decrease of relative intensity of the red band of matrix emission (635 nm) in the Yb^{3+}-doped PWO crystals.

The observed enhancement of the blue luminescence band as well as decrease of the red band are desirable for scintillation applications of the PWO crystals. We have shown in this paper that both the desirable effects of the Yb^{3+} doping on the PWO matrix emission are caused by the Yb^{3+} ions in the Pb positions. The RE^{3+} ions in the W positions in the PWO crystals are usually observed with increase of the RE impurities concentrations [13, 22–24]. Therefore, the RE ions (e.g., Yb^{3+} ions) positive effect on luminescence characteristics of the lead tungstate scintillators is expected to fall down at higher concentrations of RE impurity.

5. Conclusions

Luminescence properties of the Yb^{3+}-doped PWO crystals were studied.

Intrinsic f–f emission of two types of the Yb^{3+} centres was observed in the spectra of the Yb^{3+}-doped crystals. These centres are formed by the impurity RE ions incorporated in different positions (Pb and W sites) in the PWO crystal lattice.

The Yb^{3+} impurities influence relative intensities of the bands contributed to matrix emission. Increase of the blue band intensity is the main effect. It is supposed that first effect is caused by formation of additional Yb^{3+}-induced channel of excitons creation. Transfer of excitation energy from matrix to the Yb^{3+} emission centres

occurs in the 309–334 nm excitation range. This effect decreases intensity of the red band of matrix emission. The described influence of Yb^{3+} doping on the PWO matrix emission are caused by the Yb^{3+} ions arranged in Pb positions.

Acknowledgments

Publication is based on the research provided by the grant support of the State Fund for Fundamental Research of Ukraine. Experiments with synchrotron radiation were made at SUPERLUMI station at HASYLAB (DESY) in Hamburg.

References

[1] D. Klimm, P. Reiche, in: *Encyclopedia of Materials: Science and Technology*, Eds. K.H.J. Buschow, R.W. Cahn, M.C. Flemings, B. Ilschner, Elsevier, 2001, p. 4448..

[2] V.B. Mikhailik, H. Kraus, *Phys. Status Solidi B* **247**, 1583 (2010).

[3] P. Lecoq, *Opt. Mater.* **26**, 523 (2004).

[4] J. Wang, H. Zhang, Z. Wang, W. Ge, J. Zhang, M. Jiang, *J. Cryst. Growth* **292**, 377 (2006).

[5] Y. Huang, K. Jang, H.J. Seo, L. Zhao, *J. Korean Phys. Soc.* **49**, 227 (2006).

[6] C.E. Mungan, S.R. Bowman, T.R. Gosnell, in: *Lasers 2000*, Eds. V.J. Corcoran, T.A. Corcoran, STS Press, McLean (VA) 2001, p. 819..

[7] T.T. Basiev, A.A. Sobol, Yu.K. Voronko, P.G. Zverev, *Opt. Mater.* **15**, 205 (2000).

[8] M. Rahimi-Nasrabadi, S.M. Pourmortazavi, M.R. Ganjali, A.R. Banan, F. Ahmadi, *J. Mol. Struct.* **1074**, 85 (2014).

[9] K.V. Dabre, S.J. Dhoble, J. Lochab, *J. Lumin.* **149**, 348 (2014).

[10] X. Wang, B. Liu, Y. Yang, *Opt. Laser Technol.* **58**, 84 (2014).

[11] V.V. Laguta, M. Nikl, S. Zazubovich, *IEEE Trans. Nucl. Sci.* **55**, 1275 (2008).

[12] C.H. Yang, G. Chen, B. Wang, P.F. Shi, *Cryst. Res. Technol.* **6**, 543 (2001).

[13] S. Burachas, S. Beloglovsky, D. Elizarov, I. Makov, Yu. Saveliev, N. Vassilieva, M. Ippolitov, V. Manko, S. Nikulin, A. Nyanin, A. Vassiliev, A. Apanasenko, G. Tamulaitis, *Radiat. Meas.* **38**, 367 (2004).

[14] M.B. Kosmyna, B.P. Nazarenko, V.M. Puzikov, A.N. Shekhovtsov, *Acta Phys. Pol. A* **124**, 305 (2013).

[15] O. Chukova, S. Nedilko, V. Scherbatskyi, *Phys. Status Solidi C* **4**, 897 (2007).

[16] E. Auffray, M. Korjik, T. Shalapska, S. Zazubovich, *J. Lumin.* **154**, 381 (2014).

[17] K.W. Meert, J.J. Joos, D. Poelman, P.F. Smet, *J. Lumin.* **173**, 263 (2016).

[18] T.T. Basiev, V.N. Baumer, Yu.N. Gorobets, M.E. Doroshenko, M.V. Kosmyna, B.P. Nazarenko, V.V. Osiko, V.M. Puzikov, A.N. Shekhovtsov, *Crystallogr. Rep.* **54**, 697 (2009).

[19] Y.-L. Xu, R. Wang, B.-J. Wang, W.-H. Liu, J. Wang, M. Wang, T.-Y. Yang, *Chin. Phys. Lett.* **25**, 2246 (2008).

[20] O. Antonenko, O. Chukova, Yu. Hizhnyi, S. Nedilko, V. Scherbatskyi, *Opt. Mater.* **28**, 643 (2006).

[21] Y. Huang, W. Zhu, X. Feng, G. Zhao, G. Huang, S. Li, Z. Man, *Mater. Lett.* **58**, 159 (2004).

[22] O. Chukova, S. Nedilko, V. Scherbatskyi, *J. Lumin.* **130**, 1805 (2010).

[23] S. Novosad, L. Kostyk, I. Novosad, O. Tsvetkova, *Acta Phys. Pol. A* **117**, 143 (2010).

[24] Y. Huang, X. Feng, W. Zhu, *Appl. Phys. A* **80**, 409 (2005).

[25] O. Chukova, O. Gomenyuk, S. Nedilko, V. Polubinskii, V. Scherbatsky, V. Sheludko, Yu. Titov, *Opt. Mater.* **36**, 1709 (2014).

[26] O. Chukova, S.G. Nedilko, S.A. Nedilko, V. Scherbatsky, T. Voitenko, *Solid State Phenom.* **200**, 186 (2013).

[27] R.S. Boyko, O.V. Chukova, O.V. Gomenyuk, P.G. Nagornyi, S.G. Nedilko, *Phys. Status Solidi C* **2**, 712 (2005).

[28] A. Lupei, G. Aka, E. Antic-Fidancev, B. Viana, D. Viven, P. Aschehoug, *J. Phys. Condens. Matter* **14**, 1107 (2002).

[29] I.A. Kamenskikh, N. Guerassimova, C. Dujardin, N. Garnier, G. Ledoux, C. Pedrini, M. Kirm, A. Petrosyan, D. Spassky, *Opt. Mater.* **24**, 267 (2003).

[30] A. Matraszek, P. Godlewska, L. Macalik, K. Hermanowicz, J. Hanuza, I. Szczygieł, *J. Alloys Comp.* **619**, 275 (2015).

[31] O. Chukova, S. Nedilko, V. Scherbatskyi, *Opt. Mater.* **34**, 2071 (2012).

[32] O. Chukova, S. Nedilko, *Opt. Mater.* **35**, 1735 (2013).

[33] W. van Loo, *Phys. Status Solidi A* **28**, 227 (1975).

[34] P. Fabeni, V. Kiisk, A. Krasnikov, M. Nikl, G.P. Pazzi, I. Silidos, S. Zazubovich, *Phys. Status Solidi C* **4**, 918 (2007).

[35] P. Bohacek, N. Senguttuvan, V. Kiisk, A. Krasnikov, M. Nikl, I. Sildos, Y. Usuki, S. Zazubovich, *Radiat. Measur.* **38**, 623 (2004).

[36] M. Fujita, M. Itoh, M. Horimoto, H. Yokota, *Phys. Rev. B* **65**, 195105 (2002).

[37] M. Itoh, T. Sakurai, *Phys. Status Solidi B* **242**, R52 (2005).

[38] S. Nedilko, O. Chukova, in: *IEEE Xplore, Conf. Proc. 6912376: Int. Conf. on Oxide Materials for Electronic Engineering — Fabrication Properties and Applications*, 2014, p. 133.

[39] C. Yang, G. Chen, P. Shi, *J. Lumin.* **93**, 249 (2001).

[40] V.V. Laguta, M. Martini, A. Vedda, M. Nikl, E. Mihokova, P. Bohacek, J. Rosa, A. Hofstaetter, B.K. Meyer, Y. Usuki, *Phys. Rev. B* **64**, 165102 (2001).

[41] J.A. Groenink, H. Binsma, *J. Solid State Chem.* **29**, 227 (1979).